Plant-Derived Secondary Metabolites as Potential Mediators Against COVID-19 by MetA-Analysis, Docking, and Molecular Dynamics Methods

Afifeh Hajipour[1], Masoud Tohidfar[*1]

Received: 2023-06-19 Accepted: 2023-08-14

Abstract

Coronaviruses are viruses that often cause acute complications in the respiratory system with, symptoms similar to those of a cold. Traditions Medicine uses medicinal plants to treat various diseases, including infectious diseases. This research aims to determine the effective antiviral compounds of medicinal plants (*Glycyrrhiza glabra*, *Echinacea purpurea*, *Panax ginseng,* and *Cichorium intybus*) and the genes involved in their synthesis against coronavirus. In this study, the secondary metabolites were investigated in terms of the inhibition of COVID-19 through meta-analysis. In the database, the interaction of proteins concerning each other and hub genes was obtained from Cytoscape software. To study the ontology of genes from the Enrichr database and then Barsam HeatMap, the expression of the genes was measured relative to each other. As a result of the meta-analysis, 14 genes related to blood coagulation factors and the complement system (immune system) were determined. The compounds of medicinal plants with antiviral and antimicrobial effects were extracted from the PubChem database for docking and then checked by the HeatMap database. As a result of the meta-analysis, 14 genes related to blood clotting factors and the complement system (immune system) were found. The results obtained from the Kegg Pathway server were evaluated, and the two factors coagulation factor X (F10) and coagulation factor II thrombin (F2) as the reactivity of human cells when exposed to the virus and spike protein and main protease as the coronavirus receptor were extracted from the PDB database. Receptor (1A2C, 6lu7, 4Y79, 6VXX)-ligand docking (secondary combinations) was confirmed by the coach-d protein-ligand server. In the end, their validation was done by performing molecular dynamics using Gromax software. According to these results, by reducing the expression of thrombin factor and factor x, it prevents blood clotting, and by inhibiting the spike protein and the main protease of the Coronavirus, it prevents the multiplication of the virus using the antiviral extract of these plants.

Keywords: Sars Cov2, Microarray, Coronavirus, Drug design, Traditional herbal medicine

1-Department of Cell and Molecular Biology, Faculty of Life Sciences and Biotechnology, Shahid Beheshti University, Tehran, Iran
* Corresponding Author's email address: m_tohidfar@sbu.ac.ir
Doi: 10.48308/jpr.2024.235371.1075

Introduction

Severe acute respiratory syndrome coronavirus 2 (SARS-CoV-2) has rapidly spread worldwide, leading to the unprecedented emergence of coronavirus disease 2019 (COVID-19) on a global scale (Nuraskin et al., 2019). Coronaviruses (CoVs) cause a variety of diseases, including respiratory, intestinal, kidney, brain, and nervous diseases, in humans and animals (Nuraskin et al., 2019). The New Coronavirus 2019 (nCov2019) (recently referred to as COVID-19) appeared as a pathogen in China with initial symptoms such as fever, severe respiratory disease, and pneumonia (Tallei et al., 2020) from the beginning. Although there are no approved drugs for COVID-19, several clinical trials are underway (Hayashi et al., 2003). The SARS-CoV-2 virus has a spike (S) protein, which consists of two subunits and performs a vital part in binding to receptors and membrane of cells attachment. Scientists in all related fields are working to produce an effective vaccine or medicine for this virus around the world. Until now, some drugs have been used in the form of combined drugs to control the disease of COVID-19 in the world, but researchers are still looking for a vaccine or a special drug to treat this disease because the prescribed drugs alone are not effective in completely controlling the disease or have many side effects on body cells and tissues (Shakeran et al., 2018). Plants are one of the sources of active medicinal compounds that are widely used in the treatment of diseases caused by microbes (Shakeran et al., 2018; Earlia et al., 2019; Mustafa et al., 2019). Many of the reported bioactive plant compounds have anti-fungal, anti-bacterial, and anti-viral activities (Cheng et al., 2006, Nuraskin et al., 2020, Ou et al., 2020). Compared to conventional treatment methods, plants and plant-derived products have advantages such as simplicity, greater safety, less toxicity, lower cost, a higher speed of action, and compatibility with the environment (Huang et al., 2020). Herbal compounds, having many medicinal properties such as anti-cancer, anti-oxidant, anti-inflammatory, anti-viral, anti-bacterial, and protective of the immune system and liver, have attracted the attention of researchers. In previous studies, the potential to inhibit the multiplication of viruses and their infectiousness It has been observed (Pratiwi et al., 2015; Khwaza et al., 2018). Today, to reduce the cost and time of drug production, a lot of attention has been paid to pre-studies in drug design using bioinformatic methods. In this method, the use of bioinformatics tools and calculation methods that predict with a high confidence coefficient the effectiveness of medicinal compounds and their potential toxicity have been greatly appreciated in recent years (Benet et al., 2017; Ding et al., 2017). Molecular docking, simulation, and spot determination.

Aim and chemical stability studies are two of the most important bioinformatics methods used in drug design. Using computational methods to predict the effectiveness of pharmaceutical compounds and their physicochemical properties before the laboratory synthesis of these compounds has speeded up the process of designing pharmaceutical compounds (Huang and

Zou, 2010). According to the previously confirmed reports regarding the potential of bioactive compounds in the prevention and treatment of viral infections, several bioactive compounds known as effective drug candidates to overcome the acute symptoms of the COVID-19 virus have been investigated with the use of meta-analysis.

Material and methods

Operations of meta-analysis of transcriptome data

After downloading Series Matrix and GPL from the NCBI database, they were analyzed, and quality was measured using R software. Data quality control was done using Limma, ggplot packages, and several libraries from Bioconductor. In meta-analysis, we are faced with a problem called the test effect, which was used to remove the test effect from the COMBAT statistical method and the SVA package in the RStudio software (Wadood et al., 2013). To evaluate the correction of the testing effect, PCA was drawn after removing the batch effect in two normalization methods, COMBAT, and Quantile, and compared. Finally, the data from different experiments were merged, and a comparative analysis between treatment and control samples was done to find genes with differential expression using the LIMMA package in RStudio software.

Protein interaction network and finding hub genes

In order to identify hub genes, all genes with differential expression were determined. The STRING database contains a lot of information on protein interactions (Jensen et al., 2009). By entering the genes identified as differentially expressed genes, a protein network is drawn according to the information available in this database and provides protein connections in an output file. This output file is entered into the Cytoscape 3.8.2 software (Shannon et al., 2003), and by using the CytoHubba package and MNC algorithm, genes with the most interactions were introduced as hubs. The obtained results were presented in the form of a heatmap diagram, which was a graphic representation of data expression using colors drawn using CIMminer software (https://discover.nci.nih.gov). Pathway enrichment analysis was performed to identify the pathways in which differentially expressed genes are involved using the KEGG database (Kanehisa and Goto, 2000).

Molecular docking operations

After downloading the three-dimensional structure of the SARS-CoV-2 enzyme from the PDB database and the compounds' secondary metabolites of selected plants from the PubChem database, they were minimized in terms of energy and structure using UCSF chimera software and PyMOL. To interact with the compounds, molecular docking was used with the COACH-D method (online server). Enzyme compounds and molecules that were optimized were selected as input to the COACH website. After docking, Discovery Studio software was used to show the connection with the enzyme.

Molecular dynamics operations

The bound peptide-protein structures and their flexibility in conformation were evaluated using simulations of molecular dynamics in the YASARA mechanics

program. The AMBER14 field of forces was employed in this investigation, and the complexes with docking were sterilized first, followed by hydrogen bond orientation and optimization for experimentation.

A cubic modeling box measuring 110 × 110 × 110 A3 was stuffed with molecules of water at a concentration of 0.9899 g/cm3 and normalized with 0.9% NaCl. The TIP3P water system was utilized to solve the problem. The amino acids in the compound had their acid dissociation constant value (pKa) determined. The SCWRL methodology, paired with the use of hydrogen bond optimization in networks, was used to keep every residue of amino acids in the optimal protonation condition. The particulate mesh Ewald technique was used to determine long-range electrostatic relationships with a cutoff distance of 8 A. Maintaining the periodic boundary constraint, the simulated cell box was 20 A bigger than the peptide-protein combination to enable maximum freedom of motion. By employing the greatest descent gradient techniques (5000 cycles) with computerized annealing techniques, the energy of each computational system was reduced to the lowest possible value. For every system, a position-restrained simulation of molecular dynamics running at 80 ps was conducted at an equilibrium temperature of 310 K and pressure of 1 atm. Pressure pairing was done utilizing a manometer to perform the technique with a base pressure of 1 atm, and thermal pairing was done utilizing a Berendsen thermostat with a thermal coupling constant of 0.1 ps. 1.25 fs was selected as a duration scale for the simulation investigation. Using the SHAKE method, the chemical lengths of bonds containing hydrogen bond molecules were determined. The modeling process was permitted to run for 250 ns after achieving a state of equilibrium at 1 ns, with the simulation paths being stored every 100 ps. The RMSD, root-mean-square fluctuation (RMSF), radius of gyration (Rg), solvent-accessible surface area (SASA), and hydrogen bonds were all analyzed using the median values from the pathways, which were run three times. Moreover, binding free energy computations using MM-PBSA techniques were applied to the modeling snapshots. The MM-PBSA binding energy was computed using the YASARA macro; a positive potential suggests a better binding. The kinetics of hydrogen bonds between receptor and protein concerning time dictated the durability of ligand-protein interactions. The graphs were created using the XMgrace tool.

Examining compounds with Lipinski's law

Lipinski's law was considered for all compounds to predict the absorption rate. Lipinski's law predicts that low absorption or penetration occurs in cases where the compound in question has characteristics such as a molecular weight greater than 500 daltons, a lipophilicity factor (LogP) greater than 5, several hydrogen acceptor atoms greater than 10, and more than 5 hydrogen donor atoms. Therefore, a combination that does not have these characteristics and has Lipinski's law has more absorption and effectiveness (Leek et al., 2012).

Physicochemical properties of compounds

Having suitable physicochemical properties

makes the compound effective and selects it as a suitable drug candidate. Therefore, in this research, in addition to LogP in Lipinski, other characteristics such as solubility in water (Logs), the degree of polarity of the compound (TPSA), the degree of digestive absorption (GI absorption) of *Panax ginseng* L., *Cichorium intybus* L., *Glycyrrhiza glabra* L., and *Echinacea purpurea* compounds using the Swiss ADME server at (http://www.swissadme.ch) were investigated.

Results

quality control checks of selected samples

The quality control of the samples of different experiments with the help of a boxplot showed that all the samples of an experiment were not in the same approximate range. We converted the data to the normal state with the ComBat operation, and all the samples were in the same range (Figure 1).

meta-analysis of transcriptome data

Among the set of 4 microarray studies of control and treated with the secondary metabolites of candidate plants (*Panax ginseng* L., *Cichorium intybus* L., *Glycyrrhiza glabra* L., and *Echinacea purpurea*), which were subjected to meta-analysis, a total of 14 genes with differential expression between the control and treatment groups were identified. As shown in Table 1, several differentially expressed genes are shown.

KEGG pathway enrichment analysis

The investigation of the pathways in which differentially expressed genes are involved was done using the KEGG site, and the results showed that these genes are mostly in the coagulation and complement pathways (F2, F3, F5, F7, F8, F9, F10, F11, F12, C2, C3, C6, and C9), Coronavirus disease (C2, C3, C6, C9, and F2), *Lupus erythematosus* (C2, C3, C6, C9), Pertussis, *Staphylococcus aureus* infection, and Prion disease (C6, and C9) are involved (Figure 2).

Specifying hub genes using Cytoscape software and drawing a Heatmap diagram

To identify the key genes responding to secondary metabolites, hub gene analysis was performed on all differentially expressed genes. The STRING database contains a lot of information on interactions between proteins. By entering the genes identified as differentially expressed genes,

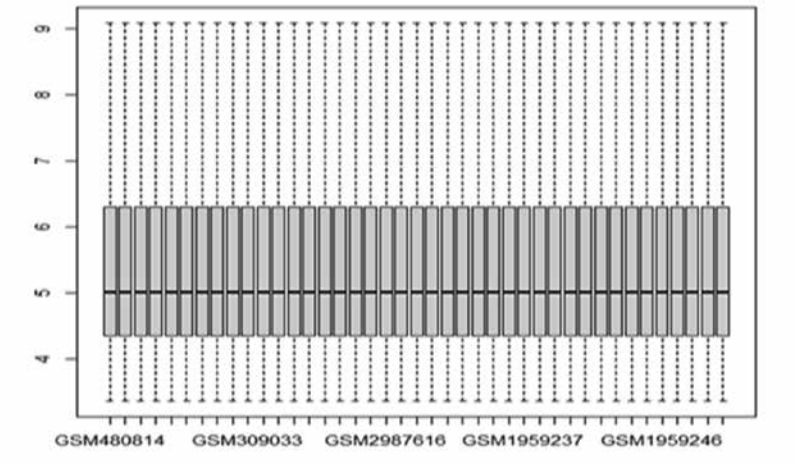

Fig. 1. Checking the quality control of the samples

Table 1. Some differentially expressed genes

Description	ID-REF	LogFC	adj.P.Val	Uniprot-ID
complement component 3 (C3)	C3	1.351037	0.126498	P01024
coagulation factor V (F5)	F5	0.553109	0.126498	P12259
coagulation factor IX (F9)	F9	0.416707	0.260081	P00740
coagulation factor X (F10)	F10	0.463198	0.33768	P00742
coagulation factor VII (F7)	F7	0.435319	0.376137	P08709
complement C9 (C9)	C9	0.211104	0.418303	P02748
coagulation factor III, tissue factor (F3)	F3	0.122006	0.814859	P13726
coagulation factor XII (F12)	F12	0.18116	0.814859	P00748
coagulation factor XI (F11)	F11	-0.54184	0.126498	P03951
complement C2 (C2)	C2	-1.24727	0.126498	P06681
complement C6 (C6)	C6	-0.73373	0.141447	P13671
T brachyury transcription factor (T)	T	-1.01159	0.141447	Q78ZW9
coagulation factor VIII (F8)	F8	-0.13741	0.814859	P00451
coagulation factor II, thrombin (F2)	F2	-0.0618	0.814859	P00734

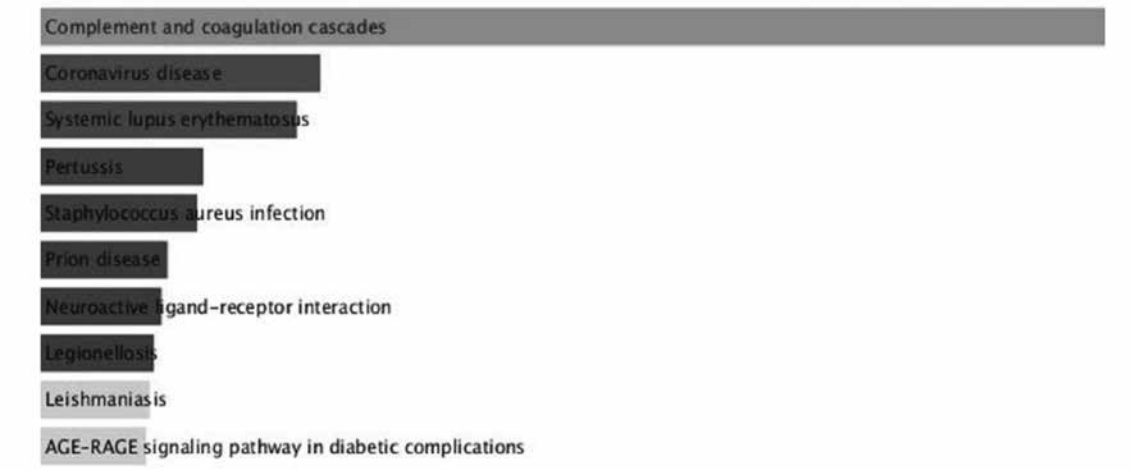

Fig. 2. KEGG pathway enrichment analysis of differentially expressed genes

a protein network is drawn according to the information in this database and provides protein connections in an output file. This output file was entered into the Cytoscape 2.8.3 software, and using the CytoHubba package and the MNC algorithm, genes with the most interactions were introduced as hubs (Figure 3). All input genes have interactions and mutual and effective relationships with each other, and the f2 and f10 genes interact with all genes. F2 and f10 genes with the most interactions were introduced as hub genes (having the most connections with other genes). Gene expression profiles often represent a vector of numerical values and usually A heatmap

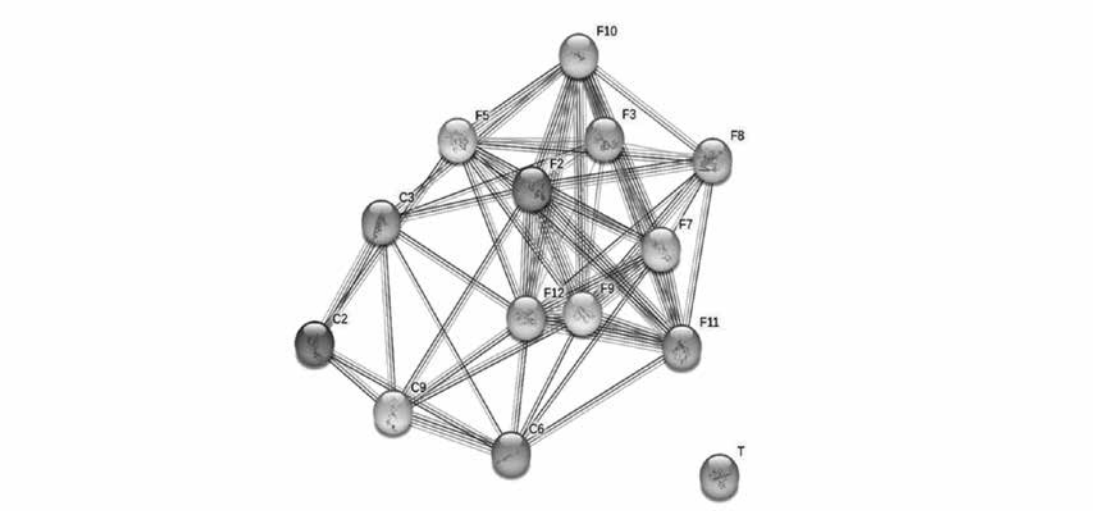

Fig. 3. Genes involved in the gene network of differentially expressed genes in the STRING database

Table 2. Hub genes identified in Cytoscape 2.8.3

Rank	1	1	3	3	5	5	7	7	9	10	10	10
Node	F10	F2	F9	F3	F8	F5	F7	F12	C6	C9	C2	C3

image (Figure 3) is shown, where the props with high expression are marked in red and the props with low expression are marked in blue (Table 2).

Heatmap drawing

The gene expression profile often represents a vector of numerical value and is usually shown with an image (Figure 4), where the high props are marked in red and the low props are marked in blue. According to the results, factor C3 is an important component in strengthening the body's immune system due to its increased expression, and factors F10 and F2, which were identified as hub genes, are the important factors of blood clotting, and their expression was reduced due to the chemical compounds of selected medicinal plants. Therefore, it was chosen as a candidate gene to prevent thrombosis caused by Coronavirus disease (Figure 4).

Molecular docking study

The results of molecular docking between plant compounds with the main protease, protein S, factor X, and thrombin factor are shown (Table 4). Among the 22 candidate herbal compounds, the inhibitory effects of glabridin, glabroisoflavanone A, paratocarpin B, and hemileiocarpin compounds had inhibitory energies of -7.8, -7.7, -7.4, and -7.3 kJ, respectively, compared to the used standard drugs. Like Remdesivir and Favipiravir, it is stronger on the main protease, with inhibition energies of -7.3 and -5.1 kJ, respectively. Next, Hemileiocarpin, Paratocarpin B, Lupeol, Glabroisoflavanone B, and Stigmasterol have inhibition energies of -6.4, -6.3, and -6.1, respectively. -5.9 and -5.8 kJ are more potent than the standard drugs Remdesivir and Favipiravir on spike protein. Hemileiocarpin, chicoric acid, beta.

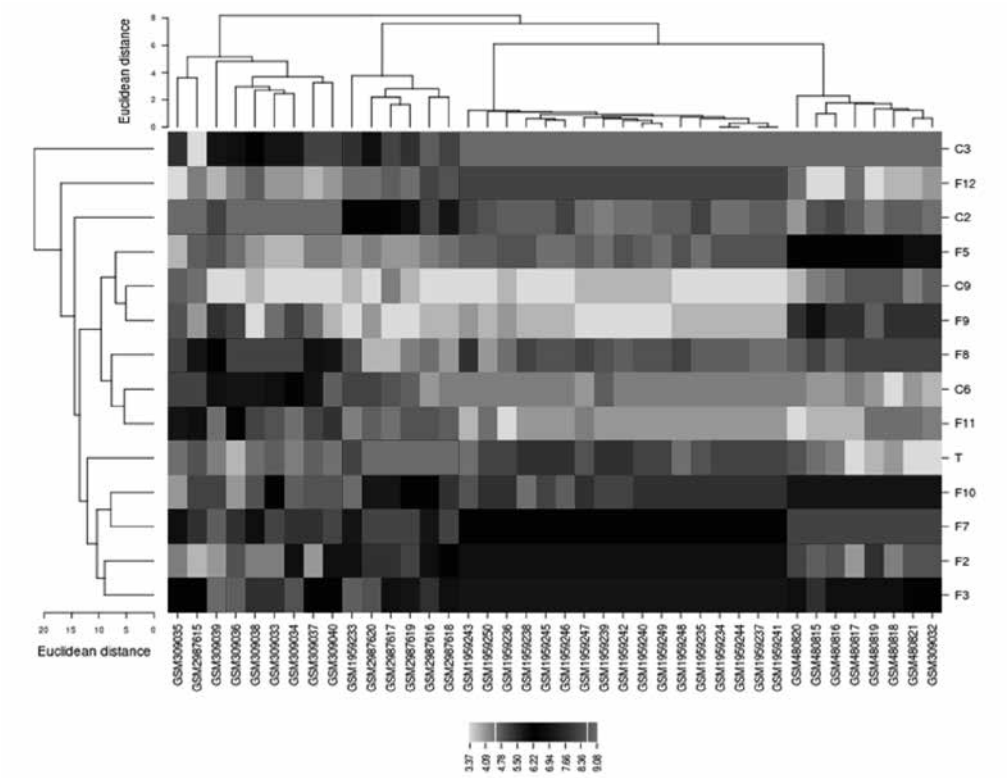

Fig. 4. Schematic of gene expression by drawing a HEAT MAP diagram

- Sitosterol and Kanzonol Y are stronger on factor X with linked energies of -9.3, -8.5, -8.5, and -8.43 kJ, respectively, than standard drugs such as Rivaroxaban with linked energies of -8.1 kJ. Stigmasterol, Paratocarpin B, Hemileiocarpin, Glabroisoflavanone A, Glabridin, and Hispaglabridin B with linked energies of -6.5, -6.3, -6.1, -5.9, -5.6, and -5.6 kJ, respectively, compared to the standard drugs used, such as Dabigatran etexilate with linked energies of -5.1 kJ, are stronger on the thrombin factor (Table 4).

Finally, the results showed that compared to the standard drugs used, the candidate herbal compounds have a suitable inhibitory power for the main protease, spike protein, and down-regulate the expression of the factor X and thrombin factor.

According to Figure 5, amino acids involved in hydrogen bonding SER185, ARG137, MET11, ASP755, SER768, and SER144 were used as key amino acids.

Examining the binding energy and ferrochemical properties of the studied drugs as a positive control

The results of the study of the drugs used as positive controls show the strong interaction of 3 of them, namely Remdesivir, Rivaroxaban, and Dabigatran etexilate, respectively, with negative linked energy of -7.3, -5.8, -8.1, and -5.1 with spike protein, main protease enzyme, factor X, and thrombin factor, respectively (Table 5). Remdesivar drug with inhibitory energy of -7.3 and -5.1 kJ has a stronger inhibitory effect due to having energy It has more negative inhibition on the main protease enzyme and spike protein, respectively. Rivaroxaban and dabigatran etexilate have stronger inhibition in terms of negative inhibition energy on factor X and thrombin factor, respectively. Among the candidate chemical drugs,

Table 4. The results of protein-ligand molecular docking

Names of herbal compounds	Energy (E) connect of 1A2C	Energy (E) connect of 4Y79	Energy (E) connect of 6vxx-RBD	Energy (E) binding of 6LU7 protein
glabridin	-5.6	-7.5	-5.5	-7.8
Glabroisoflavanone A	-5.9	-6.6	-4.1	-7.7
Paratocarpin B	-6.3	-7.5	-6.3	-7.4
Hemileiocarpin	-6.1	-9.3	-6.4	-7.3
Kanzonol Y	-5.5	-8.4	-5.7	-7.2
Glabroisoflavanone B	-4.7	-6.8	-5.9	-7.1
Chicoric acid	-4.5	-8.5	-5.5	-7.1
Chlorogenic acid	-4.9	-7.6	-4.7	-7.0
Stigmasterol	-6.5	-7.7	-5.8	-7.0
formononetion	-5.4	-6.7	-5.6	-6.9
Licochalcone C	-5.3	-7.0	-5.1	-6.7
Protopanaxadiol	-5.2	-7.0	-3.9	-6.7
Lupeol	-5.1	-6.6	-6.1	-6.7
beta.-Sitosterol	-5.1	-8.5	-4.6	-6.2
Stigmasta-5,22-dien-3-ol	-5.1	-7.7	-5.0	-6.2
Ginsenosides	-4.5	-6.9	-4.9	-6.2
Hispaglabridin B	-5.6	-6.4	-5.5	-6.0
Protopanaxatriol	-5.0	-7.1	-3.8	-6.0
Glycyrrhizic acid	-1	-3.4		-6.0
Mannopyranosyl-d-glucitol	-4.8	-7.0	-4.1	-5.7
3,4,4a,5 Tetrahydrobenzo[g]isoquinolin-10(2H)-one	-5.0	-6.7	-4.9	-5.6
Caffeic acid	-4.6	-6.1	-4.3	-5.3
Verrucarol	-4.4	-5.5	-4.7	-5.3
1R,4S,7S,11R-2,2,4,8 Tetramethyltricyclo[5.3.1.0(4,11)]undec-8-ene	-5.1	-6.4	-4.1	-5.2
5,8,11-Heptadecatriynoic acid,methyl ester	-4.2	-6.2	-4.0	-4.9
9-Octadecenoic Acid (Z)-	-3.6	-6.1	-3.9	-4.8
9,12-Octadecadienoic acid(Z,Z)-	-3.6	-6.3	-3.7	-4.7
n-Hexadecanoic acid	-3.6	-6.0	-3.9	-4.6
cis-9-Hexadecenoic acid	-3.5	-5.7	-3.8	-4.6
Tetradecanoic acid	-3.5	-5.6	-3.7	-4.3
Pentadecanoic acid	-3.4	-5.8	-3.8	-4.3
Hexadecanoic acid, methyl ester	-3.1	-5.7	-3.7	-3.9

Remdesivir, rivaroxaban, and dabigatran etexilate with the most molecular interaction and the best orientation as ligands are inside the protein complex of the virus and blood as receptors for the treatment of COVID-19 and acute symptoms (thrombosis).

Study of molecular dynamics

The simulations for Hemileiocarpin-F10, Paratocarpin B-F2, Glabridin-Main protease, and Paratocarpin B-spike protein complexes were done separately, and their results were compared (Figure 6). The simulation provided a better picture of the stability of ligands in interaction with proteins. Root-mean-square deviation (RMSD), radius of gyration (Rg), and H-bonds are used to check the stability of the model system. RMSD is a critical parameter

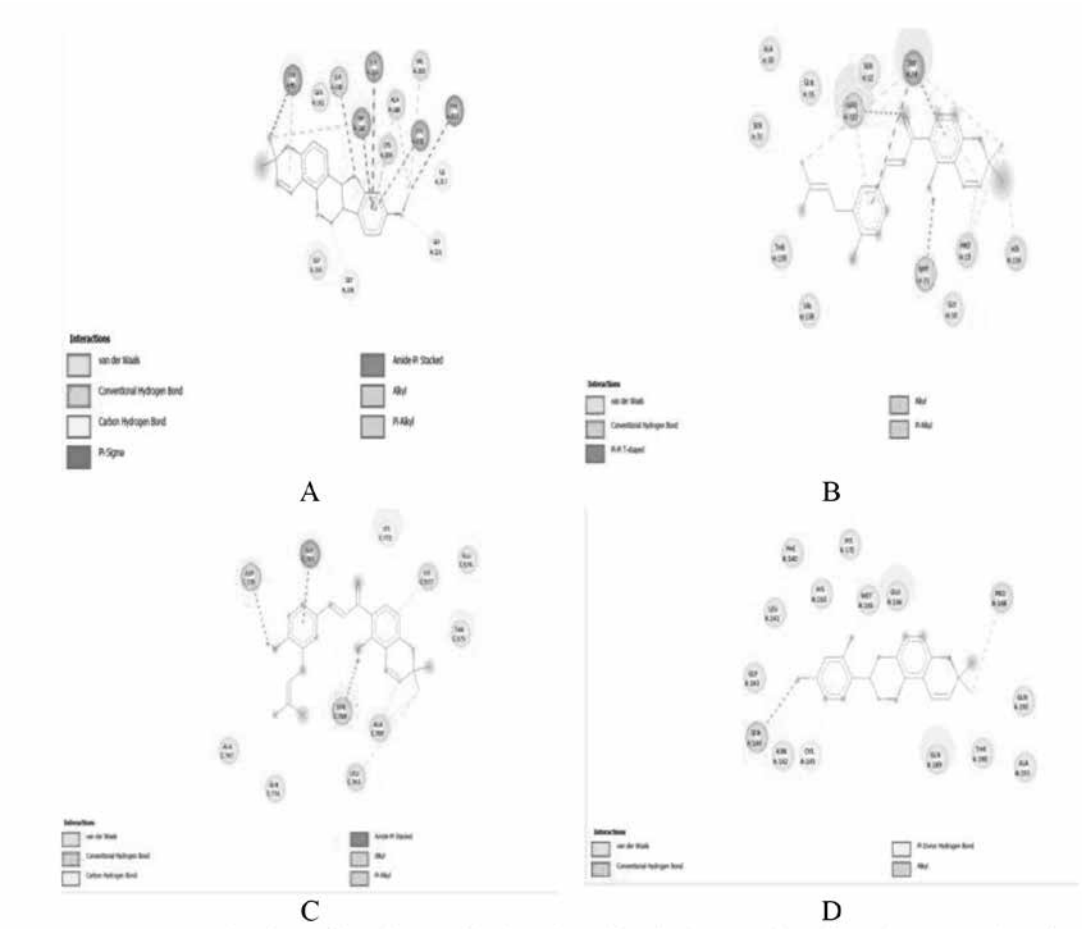

Fig. 5. Examination of amino acids involved in hydrogen bonding (green color) by Discovery studio software: A Factor X, B Thrombin Factor, C Main Virus Protease Enzyme, D Virus Spike Protein

Table 5. The physicochemical characteristics, TPSA level, solubility, and effect of drugs on vital cytochromes of the body and digestive absorption of drugs

Row	Pharmacochemical name	Access code in pubchem	Energy (E) binding of 6LU7 protein	Energy (E) connect of 6vxx-RBD	Energy (E) connect of 4Y79	Energy (E) connect of A2C	LogS	Log P	TPSA	Digestive absorption	BBB permeant	Chemical formula
1	Rivaroxaban	9875401	---	---	-8.1	---	-4.00	2.49	116.42	HIGH	NO	C19H18ClN3O5S
2	Apixaban	9875401	---	---	-7.6	---	-4.14	2.24	110.76	HIGH	NO	C25H25N5O4
3	Edoxaban	10182969	---	---	-6.0	---	-3.69	1.42	164.87	LOW	NO	C24H30ClN7O4S
4	Dabigatran etexilate	135565674	---	---	---	-5.1	-6.10	5.31	151.53	LOW	NO	C34H41N7O5
5	Warfarin	54678486	---	---	---	-4.5	-3.70	2.70	67.51	HIGH	NO	C19H16O4
6	Aspirin	2244	---	---	---	-4.2	-1.85	1.19	63.60	HIGH	NO	C9H8O4
7	Remdesivir	121304016	-7.3	-5.8	---		-4.12	1/91	213.36	LOW	NO	C27H35N6O8P
8	Favipiravir	492405	-5.1	-4.4	---		-0.80	-0.56	88.84	HIGH	NO	C5H4FN3O2

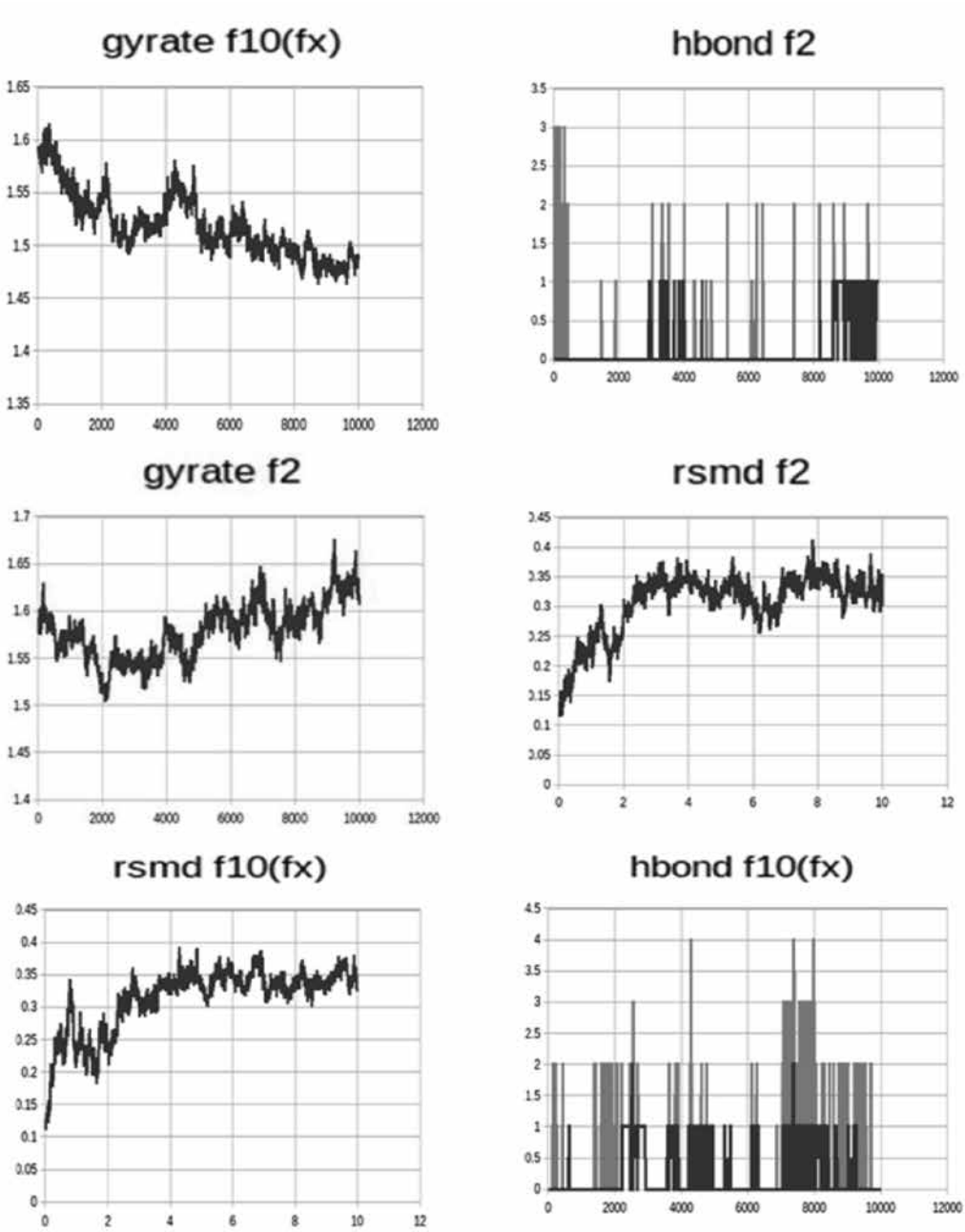

Fig. 6. RMSD and Rg diagram obtained from molecular dynamics simulation in Gromacs2022 software in a Linux environment

for MD equilibrium analysis. The RMSD of the protein backbone atoms is plotted as a function of time to check the stability of each system throughout the simulation. The RMSD values were calculated based on the simulation time scale (10 ns), and the results are shown in Figure 6. The values of RMSD have values between 0.1-0.35. From time 8 to the stability of fluctuations, it is minimized and shows stability. Intermolecular hydrogen bonding between protein and ligand plays an essential role in stabilizing the protein-ligand complex. The hemileiocarpin-F10 complex showed 1-2 hydrogen H bonds during the formation period. While the paratocarpin B-F2 complex showed a hydrogen bond during the formation period.

Discussion

In the present study, the effectiveness of the active compounds of medicinal plants, whose antiviral properties have already been confirmed in various articles, was evaluated in reducing the expression of candidate genes (f2 and f10) using meta-analysis of microarray data. The results show that these compounds can effectively reduce the expression of blood clotting factors. In this study, the evaluation of plant inhibitors in terms of physicochemical properties was evaluated by Lipinski's law using the SWISSADME online tool. This evaluation, as a basis, helps to predict the success or failure of a particular pharmaceutical or biological combination as a drug with a high probability (Balkrishna et al., 2020).

To aid in the execution of logical drug design, molecular docking techniques can be utilized to determine the binding affinity of different ligands for the target protein structure (Kanehisa and Goto, 2000). This method can help comprehend the fluctuation of interactions and possible binding processes, which can be used to apply more stringent inhibition (Nuraskin et al., 2020). Our method yielded improved structural correctness, accurate binding relationships, and affinity calculations by merging multiple docking programs and techniques (Benet et al., 2017).

A semi-flexible technique known as docking treats the ligand as a dynamic object while treating the protein's structure as a rigid entity (albeit specific remains, not the entire protein, are considered flexible). According to Khwaza et al. (2018), molecular docking is unable to replicate the physiological behavior of proteins or complexes of protein-ligand molecules. Since the majority of biological processes occur under the influence of water, MD simulation is a great and more suitable instrument for comprehending the characteristics of rigidity, adaptability, rigidity, protein-folding, and ligand-induced conformational modifications in aqueous conditions to mimic the biological roles of proteins or complexes between them (Shannon et al., 2003).

A docking investigation may shed some light on the binding locations by elucidating the relationship between binding and conformational modifications that arise during engagement. A molecular dynamics simulation can be utilized to investigate additional receptor or bound complex modifications by adjusting the pressure and temperature, which can reduce the expense of carrying out those studies in a lab setting (Nuraskin et al., 2020). The findings of docking can be validated using a combination of docking and molecular dynamics techniques (Shakeran et al., 2018). To verify the stiffness of the structure and authenticate the docking results for the structures, simulations using molecular dynamics were applied to the peptide and SARS-CoV-2 Mpro compounds. The C-alpha atoms' RMSD values were investigated to comprehend structural stiffness. According to Jiahua et al. (2020), the SASA characteristics of the peptide-protein complexes showed comparatively steady trends with little volatility, suggesting that the protein complexes did not expand or shrink throughout the modeling period.

According to Lipinski's law and the

definition of law 5, it is possible to predict the absorbability of compounds by oral route based on molecular weight, lipid affinity factor, and the number of hydrogen bond donor and acceptor atoms. Logp. It shows the amount of lipophilicity of the substance, which should be between 1 and 5 (Leif, 2020), so if its value is greater than 5, the level of lipophilicity of the substance will be greater and its digestive absorption will be less. Logs. It also shows the amount of solubility of the substance; the amount above zero indicates high solubility, and the amount less than -10 indicates the insolubility of the desired substance. Another important factor that plays a direct role in the permeability of bioactive compounds is the area of the polar parts of the molecule (TPSA) (Leif, 2020). Based on the conducted studies, the permeability of the compounds increases with the increase in mass of the substance and the decrease in PSA. Compounds that have a PSA greater than 140 angstroms do not have proper permeability. Cytochromes are important enzymes in the body that are mainly found in the liver and intestines and oxidize small foreign organic molecules such as poisons or drugs so that they can be removed from the body. Therefore, the study of these cytochromes is very effective in the absorption and effectiveness of the drug, and if the candidate compound is not an inhibitor of these cytochromes, it can be said that the drug has good digestive absorption and can be consumed orally. Finally, for the effectiveness of a drug in oral form, intravenous injection, or skin absorption, the results of the mentioned factors should be considered. According to Table No. 4, despite the high binding energy of remdesivir and dabigatran etexilate drugs, these drugs have relative solubility, poor permeability, and low gastrointestinal absorption and should be administered intravenously. However, rivaroxaban can be taken orally due to its high gastrointestinal absorption.

By considering the physicochemical characteristics of the investigated compounds, it is possible to predict the solubility, permeability, and digestive absorption of the substances for their medicinal potential. In addition to blood factors, molecular dakinase was performed on the main protease and spike virus protein against control drugs. And plant compounds Hemileiocarpin-F10, Paratocarpin B-F2, Glabridin-Main protease, and Paratocarpin B-spike protein had a stronger inhibitory effect in interaction with candidate proteins. By examining the physico-chemical properties of these compounds, they have high digestive absorption and can be used orally. Based on the results observed in this research, which was carried out to predict the decrease in the expression of factors f10 and f2, and disruption of the process of coronavirus by active plant compounds, then molecular dynamics was performed to check the stability of the designed drugs, which shows the stability of these drugs in therapeutic and interaction modes. The results of this research can be very helpful as a preliminary screening for potential medicinal candidate compounds and disease-exacerbating proteins and as a means of conducting in vitro and in vivo experiments in animal and human models.

Conclusion

According to the investigations and results, by inhibiting the spike protein (6vxx) and the main protease (6lu7) of the SARS_CoV_19 viruses and reducing the expression of thrombin factor (1a2c) and factor x (4y79) in the blood, it can be used against the Coronavirus disease. In this regard, glaberdine is the best main protease inhibitor and partocarpin B is the best spike protein inhibitor according to the lowest binding energy in the presence of the positive control drug Remdesivir, hemilocarpin to reduce the expression of coagulation factor x, and parthocarpin B to reduce the expression of thrombin factor according to the lowest energy. Transplants were selected in the presence of rivaroxaban and dabigatran etexilate, respectively.

Reference

Nuraskin CA, Idroes RM Soraya C, jufri, D. (2019). Activities inhibition methanol extract laban leaf (*Vitex pinnata*) on the growth of bacteria *S. mutans* Atcc 31987. IOP Conference Series: Materials Science and Engineering: 523 (1): p. 012008. Doi: 10.1088/1757-899X/523/1/012008.

Hayashi K, Mori M, Matsutani Y, Suzutan T, Ogasawara M, Yoshida I, Hosokawa Keizo, Tsukui A. Azuma, M. (2003). Anti-Influenza Virus Activity of a Red-Fleshed Potato Anthocyanin. Food Science and Technology Research: 9 (3): 242-244. Doi.org/10.3136/fstr.9.242.

Qian Z, Ou X, Góes LG, Osborne C, Castano A, Holmes KV, Dominguez SR. (2015). Identification of the receptor-binding domain of the spike glycoprotein of human betacoronavirus HKU1. Journal of Virology: 89(17):8816-8827. Doi. org/10.1128/jvi.03737-14.

Ren L, Wang YM. Wu ZQ, Xiang ZC, Guo L, Xu T, Jiang YZ, Xiong Y, Li YJ, Li XW, Li H, Fan GH, Gu XY, Xiao Y, Hong GH, Xu JY, Yang F, Wang XM, Wu C, Chen L, Liu YW, Liu B, Yang J, Wang XR, Dong J, Li L. (2020). Identification of a novel coronavirus causing severe pneumonia in humans: a descriptive study. Chinese Medical Journal. 133 (9):1015-1024. Doi: 10.1097/CM9.0000000000000722.

Vaira LA, Salzano G, Deiana G, De Riu G. (2020). Anosmia and ageusia: common findings in COVID-19 patients. Laryngoscope. Doi: 10.1002/lary.28692.

Recalcati S. (2020). Cutaneous manifestations in COVID-19: a first perspective. Journal of the European Academy of Dermatology and Venereology. 34 (5): 212–213. Doi:10.1111/jdv.16387.

Earlia N, Suhendra R, Amin M, Prakoeswa CRS, Idroes R. (2019). GC/MS analysis of fatty acids on Pliek U oil and its pharmacological study by molecular docking to filaggrin as a drug candidate in atopic dermatitis treatment. The Scientific World Journal. Pp 1-7. Doi: https://doi.org/10.1155/2019/8605743.

Mustafa S, Balkhy H, Gabere M. (2019). Peptide protein interaction studies of antimicrobial peptides targeting Middle East respiratory syndrome coronavirus spike protein: An In Silico Approach. Advances in Bioinformatics. p16. Doi: https://doi.org/10.1155/2019/6815105.

Shakeran Z, Nosrati M, Shakeran Z. (2018). In silico screening of hepatitis

C virus NS3/4A protease inhibitor(s) from *Cornus officinalis* and *Syzygium aromaticum*. Razi. Journal of Medical Sciences: 25(2): 69-80. Doi: 10.3390/v2081752.

Cheng PW, Ng LT, Chiang LC, Lin CC. (2006). Antiviral effects of saikosaponins on human coronavirus 229E in vitro. Clinical and Experimental Pharmacology and Physiology. 33: 612-616. Doi: https://doi.org/10.1111/j.1440-1681.2006.04415.x.

Nuraskin CA, Marlina M, Idroes RM, Soraya C, jufri D. (2020). Identification of secondary metabolite of laban leaf extract (*Vitex pinnata* L.) from geothermal areas and nongeothermal of agam mountains in Aceh Besar, Aceh province, Indonesia. Rasayan Journal of Chemistry. 13 (1): 18–23. Doi: 10.31788/RJC.2020.1315434.

Ou X, Liu Y, Lei X, Li P, Mi D, Ren L, Guo L, Guo R, Chen. T, Hu J, Xiang Z, Mu Z, Chen X, Chen J, Hu K, Jin Q, Wang J, Qian Z. (2020). Characterization of spike glycoprotein of SARS-CoV-2 on virus entry and its immune cross-reactivity with SARS-CoV. Nature Communications. 11 (1): 1620. Doi: 10.1038/s41467-020-15562-9.

Huang C, Wang Y, Li X, Ren L, Zhao J, Hu Y, Zhang L, Fan G, Xu J, Gu X, Cheng Z, Yu T, Xia J, Wei Y, Wu W, Xie X, Yin W, Li H, Liu M, Xiao Y, Gao H, Guo L, Xie J, Wang G. (2020). Clinical features of patients infected with 2019 novel coronavirus in Wuhan, China. Lancet. 395 (10223): 497-506. Doi: 10.1016/S0140-6736(20)30183-5.

Khwaza V, Oyedeji O, Aderibigbe BA. (2018). Antiviral activities of oleanolic acid and its analogues. Molecules. 23: p 2300. Doi: https://doi.org/10.3390/molecules23092300.

Pratiwi SUT, Lagendijk EL, deWeert S, Idroes R, Hertiani T, Hondel CV. (2015). Effect of *Cinnamomum burmannii* Nees ex Bl. and *Massoia aromatica* Becc. essential oils on planktonic growth and biofilm formation of *Pseudomonas aeruginosa* and *Staphylococcus aureus* in vitro. International Journal of Applied Research in Natural Products. 8 (2):1-13.

Jensen J, Kuhn M, Stark M, Chaffron S, Creevey C, Muller J, Doerks T, Julien P, Roth A, Simonovic M, Bork P, Von Mering C. (2009). STRING 8--a global view of proteins and their functional interactions in 630 organisms. Nucleic Acids Research. 37: D412–D416. Doi: https://doi.org/10.1093/nar/gkn760.

Shannon P, Markiel A, Ozier O, Baliga NS, Wang JT, Ramage D, Amin N, Schwikowski B, Ideker T. (2003). Cytoscape: a software environment for integrated models of biomolecular interaction networks. Genome Research. 13 (11): 2498-2504. Doi: https://doi.org/10.1101/gr.1239303.

Kanehisa M and Goto S. (2000). KEGG: kyoto encyclopedia of genes and genomes. Nucleic Acids Research. 28 (1): 27–30. Doi.org/10.1093/nar/28.1.27.

Jiahua H, Huanyu T, Yumeng Y, Sheng-You H, Xiao Yi. (2020). Molecular mechanism of evolution and human infection with the novel coronavirus (2019-nCoV). bioRxiv preprint Doi: https://doi.

org/10.1101/2020.02.17.952903.

Diao K, Han P, Pang T, Li Y, Yang Z. (2020). HRCT Imaging Features in Representative Imported Cases of 2019 Novel Coronavirus Pneumonia. Precision Clinical Medicine. 3 (1): 9-13. Doi: 10.1093/pcmedi/pbaa004.

Wang N, Shi X, Jiang L, Zhang S, Wang D, Tong P, Guo D, Fu L, Cui Y, Arledge KC, Chen YH, Zhang L, Wang X. (2013). Structure of MERS-CoV spike receptor-binding domain complexed with human receptor DPP4. Cell Research. 23: 986–993. https://doi.org/10.1038/cr.2013.92.

Balkrishna A, Pokhrel S, Singh J, Varshney A. (2020). Withanone from *Withania somnifera* may inhibit Novel Coronavirus (COVID-19) entry by disrupting interactions between the viralS protein receptor binding domain and host ACE2 receptor. Virology. 1-26. Doi: https://doi.org/10.2147/DDDT.S292805.

Tallei TE, Tumilaar SG, Niode NJ, Wali F, Kepel BJ, Idroes R, Effendi Y. (2020). Potential of Plant Bioactive Compounds as SARS-CoV-2 Main Protease (Mpro) and Spike (S) Glycoprotein Inhibitors: A Molecular Docking Study. Scientifica. P. 18. Doi.org/10.1155/2020/6307457.

Benet LZ, Hosey CM, Ursu O, Oprea TI. (2017). BDDCS, the rule of 5, and Drugability. Advanced Drug Delivery Reviews. 1: 101: 89-98. Doi: 10.1016/j.addr.2016.05.007.

Ding Y, Cao Z, Cao L, Ding G, Wang Z, Xiao W. (2017). Antiviral activity of chlorogenic acid against influenza A (H1N1/ H3N2) virus and its inhibition of neuraminidase. Scientific Reports. 7: 45723. Doi: https://doi.org/10.1038/srep45723.

Huang SY, Zou X. (2010). Advances and challenges in protein -ligand docking. International Journal of Molecular Sciences. 11 (8): 3016 -34. Doi: 10.3390/ijms11083016.

Wadood A, Ahmed N, Shah L, Ahmad A, Hassan H and Shams S. (2013). In -silico drug design: An approach which revolutionarised the drug discovery process. OA Drug Design and Delivery. 1 (1): 3 - 7.

Leek JT, Johnson WE, Parker HS, Jaffe AE, Storey JD. (2012). The sva package for removing batch effects and other unwanted variations in high-throughput experiments. Bioinformatics. 28 (6):882–883. Doi: https://doi.org/10.1093/bioinformatics/bts034.

Lipinski CA. (2000). Drug-like properties and the causes of poor solubility and poor permeability. Journal of Pharmacological and Toxicological Methods. 44 (1): 235 - 49.

Zoete V, Cuendet MA, Grosdidier A. (2011). Michielin Swiss Param: a fast force field generation tool for small organic molecules. Journal of Computational Chemistry. 32 (11): 2359-2368. https://doi.org/10.1002/jcc.21816.

Leif EP. (2020). COVID-19 and Flavonoids: In Silico Molecular Dynamics Docking to the Active Catalytic Site of SARS-CoV and SARSCoV-2 Main Protease. Doi: 10.13140/RG.2.2.22294. 50246.